

Centimeter-Level Indoor Visible Light Positioning

Zhu, Ran; Van Den Abeele, Maxim; Beysens, Jona; Yang, Jie; Wang, Qing

DOI

[10.1109/MCOM.002.2300296](https://doi.org/10.1109/MCOM.002.2300296)

Publication date

2024

Document Version

Final published version

Published in

IEEE Communications Magazine

Citation (APA)

Zhu, R., Van Den Abeele, M., Beysens, J., Yang, J., & Wang, Q. (2024). Centimeter-Level Indoor Visible Light Positioning. *IEEE Communications Magazine*, 62(3), 48-53.
<https://doi.org/10.1109/MCOM.002.2300296>

Important note

To cite this publication, please use the final published version (if applicable).
Please check the document version above.

Copyright

Other than for strictly personal use, it is not permitted to download, forward or distribute the text or part of it, without the consent of the author(s) and/or copyright holder(s), unless the work is under an open content license such as Creative Commons.

Takedown policy

Please contact us and provide details if you believe this document breaches copyrights.
We will remove access to the work immediately and investigate your claim.

Green Open Access added to TU Delft Institutional Repository

'You share, we take care!' - Taverne project

<https://www.openaccess.nl/en/you-share-we-take-care>

Otherwise as indicated in the copyright section: the publisher is the copyright holder of this work and the author uses the Dutch legislation to make this work public.

Centimeter-Level Indoor Visible Light Positioning

Ran Zhu, Maxim Van den Abeele, Jona Beysens, Jie Yang, and Qing Wang

The authors propose a data pre-processing method in visible light positioning systems — including data cleaning and data augmentation — to construct reliable and dense fingerprint samples, thereby alleviating the impact of noisy samples as well as reducing labor intensity.

ABSTRACT

Visible light positioning (VLP) based on the received signal strength (RSS) can leverage a dense deployment of LEDs in future lighting infrastructure to provide accurate and energy-efficient indoor positioning. However, its positioning accuracy heavily depends on the density of collected fingerprints, which is labor-intensive. In this work, we propose a data pre-processing method, including data cleaning and data augmentation, to construct reliable and dense fingerprint samples, thereby alleviating the impact of noisy samples as well as reducing labor intensity. Extensive experiments demonstrate that our proposed method achieves an average positioning error of 1.7 cm, utilizing a sparse dataset that reduces the fingerprint collection effort by 98 percent. Running a tinyML-based model for VLP on the Arduino Nano microcontroller, we also show the possibilities for deploying RSS fingerprint-based VLP systems on resource-constrained embedded devices for real-world applications.

INTRODUCTION

While the global positioning system (GPS) is the de facto solution for outdoor positioning, the research for an equally pervasive solution for indoor positioning has remained intangible, despite extensive academic research and significant commercial value [1]. A large number of applications, such as smart retail and navigation through large public facilities like hospitals, shopping malls, assisted living in smart homes, and mechanical arm tracking in the industrial sectors, have led to exploring different wireless technologies including WiFi [2], Bluetooth [3], Zigbee [4], and ultra-wideband [5], for indoor positioning. Although such approaches have been developed for a long time, they still have limitations regarding low accuracy, electromagnetic interference, and crowded spectrum resources [6]. The rapid adoption of the light emitting diode (LED) for illumination and the advancement of visible light communication (VLC) technology have made visible light positioning (VLP) a promising candidate for indoor positioning applications because it can 1) leverage pervasively available lighting infrastructure, 2) has notable positioning accuracy, and 3) has high-security characteristics. Also, LED light is in the license-free spectrum band, and safe for humans, which is especially interesting for operating rooms in hospitals where the appearance of radio frequen-

cy (RF) signals is potentially harmful to patients and diagnostic devices. Furthermore, the influence of multi-path reflection on positioning accuracy is not as significant as in the case of RF [7].

To develop a VLP system, a variety of technologies have been proposed including angle-of-arrival (AOA) [8], time-of-arrival (TOA), time-different-of-arrival (TDOA) [9], and received signal strength (RSS) [10]. AOA can achieve good position estimation but relies on high computational complexity and expensive equipment. TOA and TDOA require sensitive hardware at the receiver and also need perfect synchronization between transmitters and receivers. RSS-based positioning can be achieved with cost-effective hardware without requiring any synchronized infrastructure. Typically, multiple LEDs are used as transmitters, whereas photodiodes (PDs) or a camera act as the receiving terminal in the VLP system. The lower price and power costs make PDs preferable for universal applications.

In this work, we use RSS-based fingerprinting to achieve an effective and accurate VLP on microcontrollers, empowered by tiny machine learning (TinyML). One of the advantages of machine learning (ML) algorithms is that prior knowledge of the physical model for VLP is not a prerequisite, as it is commonly embedded within the training set. As such, we develop an RSS-based fingerprinting VLP system where a variety of RSS fingerprints are built from different positions and stored in the database as a training set carried out by the offline phase, and the location is determined by means of new RSS measurements for the online phase. We propose the data cleaning and data augmentation strategies to relieve the burden of data collection and build reliable dense VLP fingerprints.

CHALLENGES IN RSS-BASED VLP

For data-driven RSS-based VLP methods empowered by ML, one important requirement is the density and quality of labeled fingerprints or anchors directly influence the final performance of VLP. Thus, the first challenge in RSS-based VLP is *how to provide reliable dense VLP fingerprints over a wide area?* To address this challenge, we leverage our dense LED testbed of 36 transmitters and 4 receivers with off-the-shelf devices (Fig. 1), provide centimeter-level RSS fingerprints at 351,384 locations, and evaluate it with extensive

Ran Zhu, Jie Yang, and Qing Wang are with Delft University of Technology, The Netherlands; Maxim Van den Abeele is with KU Leuven, Belgium; Jona Beysens is with the Swiss Center for Electronics & Microtechnology, Switzerland.

Digital Object Identifier: 10.1109/MCOM.002.2300296

and realistic experimental setups. However, those collected RSS data recorded by PDs always contain noise due to the device's thermal noise or sampling noise. To solve this problem, we propose a data-cleaning strategy to confront noisy RSS by leveraging three measurements at each position and performing interpolation using surrounding RSS information to obtain more reliable and accurate results.

High-performance RSS fingerprint-based positioning methods benefit from the dense collected data while collecting high-quality labeled fingerprints is labor-intensive. Therefore, to increase the applicability and performance of methods, the second challenge is *how to build the high-granularity RSS fingerprint database with limited manual involvement?* Most fingerprinting-based localization systems [11, 12], which aim at addressing the need for offline measurements, purely rely on the simulation to construct the offline fingerprint map and compare the online RSS readings with RSS readings stored in the database for localization. However, simulating the fingerprint map of light intensity distributions using a simplified analytical model of LED illumination patterns lacks realism due to the absence of background noise and various reflections involved. In this article, we propose a data augmentation strategy, as an alternative solution, to relieve the burden of data collection.

However, traditional ML technologies typically require large amounts of computational resources and memory, limiting their applicability on resource-constrained embedded platforms. As on-device intelligence becomes increasingly important with the rise of edge computing in the internet of things (IoT), the next challenge is *to enable practical and implementable ML systems on resource-constrained devices.* To tackle this challenge, we deploy our ML-based positioning system on the Arduino Nano BLE 33, an embedded platform with limited computational resources. To further expedite the realization, we utilize TinyML, empowered by the model compression technique, to enable intelligent decision-making at the edge.

BUILDING AND OPTIMIZING THE RSS DATASET

RSS fingerprint-based VLP has been extensively studied, based on data from either simulation [11, 12] or testbed [13, 14]. However, most of the reported datasets are much smaller than those encountered in real-world environments, both in terms of testbed size and sampling data volume, making it difficult to assess the practical applicability of their findings. In this section, we provide a new high-granularity RSS dataset from our testbed and detail the process of how we obtain reliable data points.

DATA ACQUISITION

We implement the system based on our DenseVLC testbed with off-the-shelf devices for data collection. The entire setup is depicted in Fig. 1. This system includes 36 LED transmitters (TXs) and 4 receivers (RXs). The TXs are mounted on a height-adjustable ceiling in a 6×6 array with an inter-TX distance of 0.5 m. We use the high-performance LED CREE XT-E, covered by the lens TINA FA10645 to limit the field of the view of the LED. An NTR4501 power transistor is used to drive the LED. The RXs are placed on the floor, controlled by 4 OpenBuilds ACRO Systems.

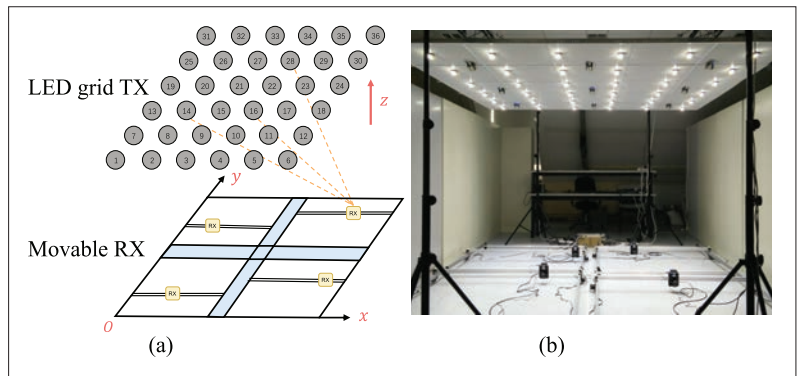


FIGURE 1. The setup to obtain our high-granularity RSS dataset for VLP from our testbed which has $6 \times 6 = 36$ LED transmitters: a) illustration and b) testbed.

Each RX is equipped with a photodiode S5971. A low-noise trans-impedance amplifier OPA659 amplifies the photodiode current to a voltage. We use the analog-to-digital converter ADS7883 to digitize the signal and send it to the embedded computer BeagleBone Black for further processing. The whole area on the floor, with the size of $3 \text{ m} \times 3 \text{ m}$, is divided into 4 square grids with a cross-like gap in the middle. Each grid covers an accessible area of approximately $1.2 \text{ m} \times 1.2 \text{ m}$, where the movement of the corresponding RX along the track can be decomposed into x and y directions.

Based on the data collection setup described above, each sampling fingerprint in the dataset comprises the RSS values from 36 LEDs and the corresponding x, y, and z coordinates of the measurement position. We use $I_{x,y,z}^j$ to denote the RSS value of LED j captured at sampling position $p = (x, y, z)$, in which $j \in \{1, \dots, C\}$, and C denotes the number of LEDs. The measurements are conducted at 1 cm intervals in both the x and y directions, resulting in a dataset with a size of 351,384 samples. Specifically, for each RX at a specific height, there are 121 steps in the directions of both x and y. Note that in this article, we focus on 2D localization. Without the loss of generality, the measurements are taken at two different heights (the vertical distance between the TX and the RX): 172 cm and 196 cm. At every sampling position, the measurement is repeated three times.

DATA CLEANING

In Fig. 2(●), we observe some abnormal readings within the collected data. The unstable device, sampling noise, and varying ambient light may corrupt the PDs' reading, which highlights the essential of data cleaning to remove these outliers. To this end, we propose a two-stage data-cleaning method. In the first stage, the fingerprint sample that best fulfills the continuity requirement of light intensity is retained out of three trials to maximize the retention of authentic environmental information. If the first stage fails to select the appropriate measurement at the target position, the second stage is activated, using the values of nearby data points to estimate the value at the missing or erroneous point.

The metric that evaluates the accuracy and consistency of the data is established by comparing the continuity of RSS values at the target position with those from the surrounding fingerprints, which is described by the following equation:

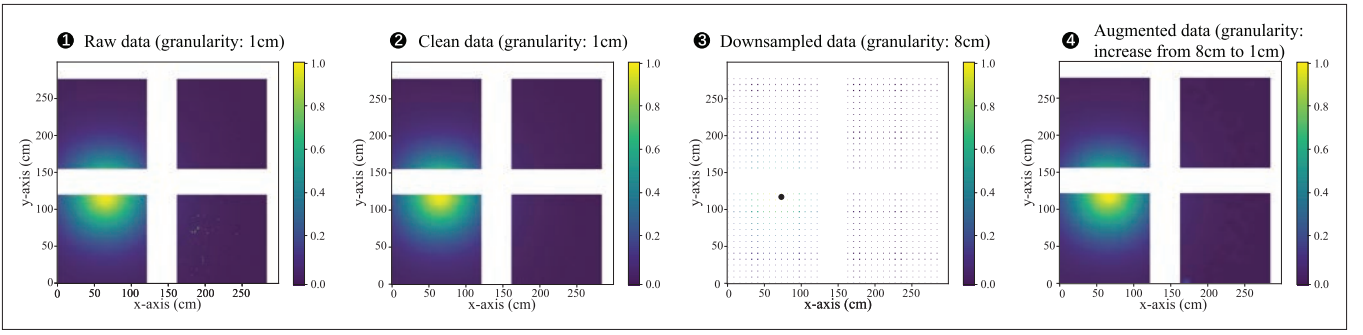


FIGURE 2. The visualization of light intensity emitted from the LED with index/ID 14 in different steps of data process. The black dot (highlighted in ③ and omitted in other sub-figures) indicates the projection of this LED onto the 2D floor plane. The augmented data (④) of 1 cm granularity is obtained from coarse sampling points with 8 cm intervals shown in ③. The color bar denotes the normalized light intensity.

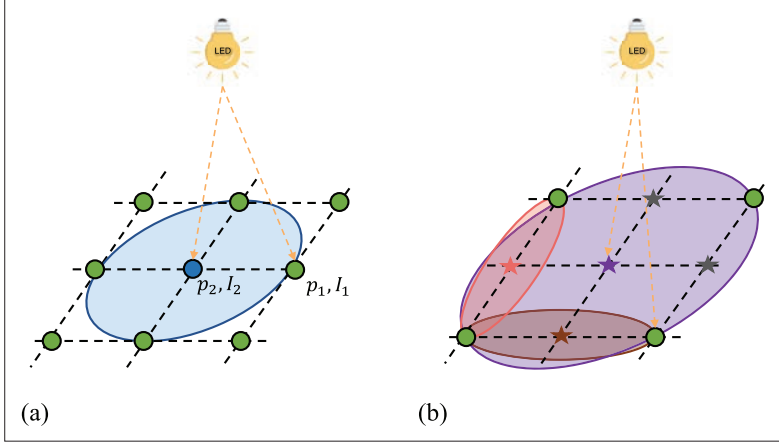


FIGURE 3. The illustration of the: a) data cleaning process; b) data augmentation process. The green circle denotes the locations of known RSS values. The blue circle and star indicate the locations to be cleaned and interpolated, respectively.

$$\Delta I_{x,y} = \left| I_{x,y} - \frac{1}{|I_s|} \sum_{I \in I_s} I \right|, \quad (1)$$

where $\Delta I_{x,y}$ is the difference between the RSS value $I_{x,y}$ at position (x, y) and the average RSS value from surrounding sampling points I_s . We consider the RSS value $I_{x,y}$ to be consistent when $\Delta I_{x,y}$ is small enough to approach 0.

For the data interpolating in the second step of data cleaning, we follow the Lambertian model. The intensity of emitted light from an LED is modeled by the Lambertian model [15]:

$$I^r = \begin{cases} I^t A(d) \cos^m(\phi) \cos(\psi), & 0 \leq \psi \leq \psi_c \\ 0, & \text{otherwise} \end{cases}, \quad (2)$$

where I^t is the lamp emission power, ψ is the incident angle, ψ_c is the FoV of the LED lamp, ϕ is the irradiation angle, $m = \frac{-\ln(2)}{\ln(\cos(\phi_{1/2}))}$ is the LED's Lambertian order in which $\phi_{1/2}$ denotes the half power semi-angle, $A(d)$ is a propagation loss function on distance d between the TX and RX. For fingerprints in each grid of the data collection testbed captured by the same PD on the same plane, we can assume $\phi = \psi$.

For the pair of points $p_1 = (x_1, y_1, 0)$ and $p_2 = (x_2, y_2, 0)$ as shown in Fig. 3, their RSSs I_{x_1, y_1}^r and I_{x_2, y_2}^r follow the model in Eq. 2. Considering that the time consumed during the process of data acquisition is much smaller than the lifetime of j th LED with the known location which can be

neglected, we assume that the LED emission power remains stable when PD collects the light intensity coming from this LED at different locations. By comparing their RSSs, we have the following ratio:


$$\frac{I_{x_1, y_1}^r}{I_{x_2, y_2}^r} = \frac{A(d_1)}{A(d_2)} \left[\frac{\cos(\phi_1)}{\cos(\phi_2)} \right]^{m+1}, \quad (3)$$

where d_i can be easily obtained from the known locations of the corresponding LED and target points, $\cos \phi_i = z_{led}/d_i$. The noisy RSS values that need to be cleaned can be easily obtained according to Eq. 3 by utilizing the reference fingerprints in I_s . We use the mean of the clean RSS values calculated from reference fingerprints as the final RSS values at the target location. As shown in Fig. 2(②), the above functions provide a solution to ensure that the data is as accurate and complete as possible, retaining real sampling points while employing the data cleaning strategy to compensate for missing or erroneous data.

DATA AUGMENTATION

For data augmentation, our objective is to generate a dataset with high-granularity fingerprints that can achieve centimeter-level positioning accuracy. Specifically, we aim to construct the 1 cm granularity dataset from sparse fingerprints such as 8 cm. To this end, we divide the interesting positioning area of the testbed into equal grid cells of 1cm square and collect RSS values at known positions with a large spacing of 8 cm along the x and y axes, respectively. The collected RSS values form a square-shaped layout, which serves as the basis for generating fingerprints with 1 cm granularity. We use the adjacent collected RSS values to interpolate the RSS values at points without measurements by utilizing the Lambertian radiation model (i.e., Eq. 3), reducing the number of required measurements while maintaining high accuracy. As shown in Fig. 3, instead of fixing the number of nearest points, we utilize the best nearest points so that reflections and the characteristics of LEDs can be taken into account in the interpolation process.

To summarize, the data optimizing process first carries out the data cleaning on raw fingerprints while maintaining the granularity. Data augmentation can be then employed to further enhance the granularity. In this way, the data collection overheads can be ameliorated up to 98 percent when we augment the 8 cm coarse



Conf	Random forest			SVM			MLP		
	Raw	Clean	Augmented	Raw	Clean	Augmented	Raw	Clean	Augmented
Conf 1	0.97	0.44 _{↓54.6%}	1.37 _{↑41.2%}	3.94	1.14 _{↓71.1%}	1.30 _{↓67.0%}	2.23	1.43 _{↓35.9%}	1.71 _{↓23.3%}
Conf2	2.38	0.79 _{↓66.8%}	2.18 _{↓8.4%}	14.41	6.25 _{↓56.6%}	6.41 _{↓55.5%}	3.11	1.14 _{↓63.3%}	2.07 _{↓33.4%}
Conf3	42.45	6.89 _{↓83.8%}	9.30 _{↓78.1%}	55.76	31.31 _{↓43.8%}	31.23 _{↓44.0%}	42.06	7.05 _{↓83.2%}	8.84 _{↓79.0%}
Conf4	1.22	0.57 _{↓53.3%}	1.77 _{↑45.1%}	7.13	3.57 _{↓50.0%}	3.57 _{↓50.0%}	2.54	1.61 _{↓36.6%}	2.15 _{↓15.4%}
Conf5	2.40	1.74 _{↓29.2%}	4.35 _{↑81.3%}	22.91	18.10 _{↓21.0%}	18.03 _{↓21.3%}	4.67	2.80 _{↓40.6%}	3.91 _{↓16.3%}
Conf6	10.55	3.20 _{↓69.7%}	4.49 _{↓57.4%}	42.71	36.46 _{↓14.6%}	36.22 _{↓15.2%}	11.26	3.89 _{↓65.5%}	5.13 _{↓54.4%}

TABLE 1. The average positioning error (cm) under various data sources using three positioning methods for different TX topologies. Augmented data is interpolated based on 8 cm-interval fingerprints. The left figure indicates the proposed LED configurations. LEDs encircled by a certain color are included in that particular configuration.

fingerprints (Fig. 2(ⓐ)) to a 1 cm fine granularity (Fig. 2(ⓑ)). In our experimental settings, these coarse fingerprints are obtained by downsampling the dense clean data (Fig. 2(ⓐ)) derived from the proposed data-cleaning strategy. To evaluate the effectiveness of this approach, we compute the mean absolute percentage error (MAPE) of the RSS values between the clean data and the augmented data and yield an error of 4.9 percent, indicating that the augmented dense data closely approximates the real one.

EXPERIMENTAL EVALUATION

EXPERIMENTAL SETTINGS

Dataset: To avoid the biases arising from differences in the magnitude of the data and stabilize the training process of ML techniques, we use the min-max scaling data normalization method to scale each data sample $I_{x,y}$ to a range between 0 and 1 by subtracting the minimum RSS value from each data point and then dividing by the range (i.e., the difference between the maximum and minimum RSS values). In this way, the j th RSS value of normalized data sample $I_{x,y}$ can be obtained. Then, all normalized data samples are randomly split into training, testing, and validation sets, accounting for 70 percent, 20 percent, and 10 percent, respectively.

Positioning Methods: We evaluate the proposed data cleaning and data augmentation strategies on the following common state-of-the-art machine learning techniques: support vector machine (SVM), random forest, and multi-layer perception (MLP). SVM and random forest are trained using the scikit-learn framework. Note that there is no tuning on these models for the simple comparison. We employ a five-layer MLP, with 256, 512, 1024, 512, and 256 hidden units respectively, and the Adam optimizer with the learning rate $1e-4$ for gradient descent.

Positioning Error: We take Euclidean distance error E_p of the x-y 2D plane between the predicted position and ground truth as metric. In this article, we adopt the average positioning error and the average of the top-90 percent positioning errors to evaluate the positioning performance. Besides, we leverage the cumulative distribution function (CDF) of positioning errors and 90th percentile error bound to detail the error distribution.

PERFORMANCE UNDER VARIOUS TXS CONFIGURATIONS

The LED topology figure in Table 1 presents the common arrangements of LEDs, featuring differ-

ent densities that can be easily replicated and implemented in practical settings. It can be clearly observed that the positioning error completely relates to the TX densities. Among three ML technologies applied to the same LED configuration, random forest demonstrates the best positioning performance, followed by MLP with a slightly higher positioning error, while SVM performs the worst in all three data sources. This phenomenon can be attributed to SVM's suitability for linear problems, while the VLP task involves the non-linear relationship between the light intensity of multiple LEDs and the target location. Additionally, random forest's robustness to outliers and noise through the aggregation of decision tree votes is evident in Table 1, where it outperforms the other methods, particularly with raw data compared to clean and augmented data. MLP often suffers from overfitting and computational complexity, negatively affecting its performance. These findings highlight the potential of random forest and MLP for RSS fingerprint-based VLP applications. Depending on specific requirements, random forest could be preferable for faster training or limited training data, while MLP is better suitable for scenarios with more complex mapping relationships and massive data.

The results from three data sources also show that positioning accuracy can be significantly improved by utilizing clean data as training data. This demonstrates data cleaning strategy plays a crucial role in improving the positioning performance of all methods across all LED configurations. Specifically, the positioning error can be decreased up to 83.8 percent in Conf 3 leveraging random forest. Besides, augmented data usage substantially decreases the average positioning error for each method, compared to using raw data directly. This is because augmented data is generated by downsampling dense clean data (1 cm) to produce sparse clean data (8 cm), which is then augmented to 1cm-granularity dense data using our proposed strategy. When deploying random forest for positioning, adopting augmented data still greatly improves the positioning performance even for sparse LED topologies such as Conf 2, 5, and 6. For dense LED configurations (Conf 1, 3, 4), augmented data results in a slightly higher positioning error compared to raw data, while this can be offset by the advantage of reducing fingerprint collection effort by 98 percent. These results strongly support the effectiveness of our data augmentation strategy in achieving a balance between positioning accuracy

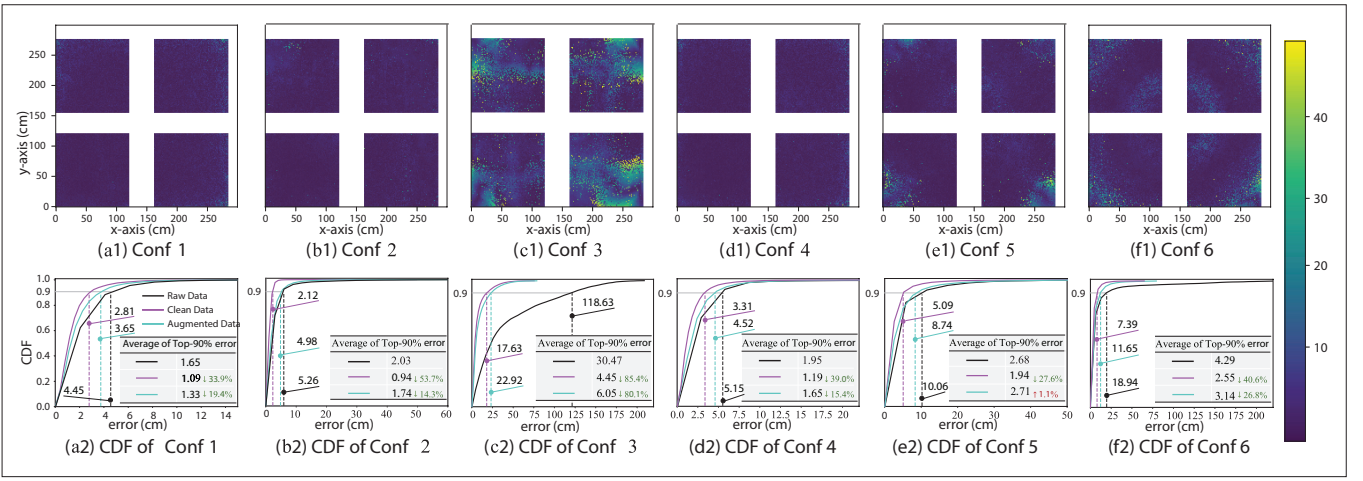


FIGURE 5. The heatmap and the CDF of positioning errors using the MLP method for different TX configurations: representing the performance on various LED topologies. To effectively visualize the positioning performance patterns, the displayed 2D error is color-coded within an interval of 0 to 50 cm. The dashed curves denote the corresponding 90th percentile errors.

Conf	Downsampling Interval					
	8 cm		4 cm		2 cm	
	AE	Top-90%	AE	Top-90%	AE	Top-90%
Conf 1	2.67	0.78	1.35	0.59	1.14	0.34
Conf 2	2.79	1.13	2.19	0.76	1.93	0.48
Conf 3	10.46	9.02	9.31	8.25	8.79	7.43
Conf 4	4.07	2.30	3.33	1.33	2.68	0.67
Conf 5	6.77	2.27	4.63	1.69	3.20	0.79
Conf 6	7.54	6.72	5.64	3.99	4.23	3.51

TABLE 2. The positioning error of 1 cm-granularity augmented data under various data downsampling rates running MLP method on the embedded device for different TX configurations. AE and Top-90% indicate the average error and the average of the top-90% errors (cm), respectively.

cy and fingerprint collection density.

In addition, we create heatmaps to visualize MLP's positioning performance. The positioning error for each position that can be reached in the testbed is color-coded and displayed, as shown in Fig. 4. There is no need for a TX configuration as dense as Conf 1, as even TX Conf 2 performs well with half the density. Therefore, there is potential for further reducing the density of TXs. This is due, in part, to the presence of a lens mounted on the LEDs in our setup, which focuses the beam of light. We also observe that the heatmap in Conf 6 shows an accurate prediction can be made within a radius of approximately 1.5 meters around a 2×2 TX grid. However, Conf 3 cannot yield reliable predictions. This can be linked to the distance between the TXs where 1.5 meters distance is obviously too large. These results guide LED grid density for target positioning accuracy. We show the CDF of positioning errors and the average of top-90 percent positioning errors for six TX configurations. The results reveal that the performance of augmentation obtained from sparse fingerprint collection is very close to that from dense clean data, and both outperform the positioning accuracy of raw data. Furthermore, we provide the 90th percentile error, underscoring that the majority of positioning errors are below 6 cm under a dense deployment of LEDs. Errors tend to increase for sparse LED deployments like Conf

3 and Conf 6. However, even in the case of Conf 3 with the most dispersed LED deployment, leveraging augmented data leads to an 80.6 percent reduction in the positioning error, from 118.6 cm to 22.9 cm, compared to using the raw data.

PERFORMANCE UNDER RESOURCE-CONSTRAINED SCENARIOS

The demand for highly intelligent edge devices in artificial IoT has been increasing significantly. This trend forces learning models deployed on resource-constrained microcontrollers to achieve low power consumption, real-time processing, and reduced latency. We employ TensorFlow Lite Micro to obtain a quantitative model and evaluate its performance on the Arduino Nano, a popular embedded platform with a small form factor and low power consumption. The quantization process reduces the model size from 5.3 MB to 1.27 MB, leading to a significant improvement in the model size and runtime, albeit with a slight increase in positioning error compared to the full-sized model. Detailed analysis of the quantitative model's positioning error is presented in Table 2, where augmented data with varying sampling intervals are used for training. The results demonstrate a decrease in positioning accuracy as the downsampling interval increases. However, our proposed data cleaning and data augmentation strategies successfully enable the VLP system to maintain high positioning accuracy even at large downsampling intervals. Based on these findings, our proposed approach holds promise in enabling the development of highly efficient and accurate VLP on embedded devices.

CONCLUSION

In this article, we proposed data cleaning and augmentation methods to achieve centimeter-level indoor visible light positioning (VLP). By evaluating our methods on Arduino Nano, we show the possibilities of achieving an RSS fingerprint-based centimeter-level VLP on resource-constrained embedded devices, which can be used in the future for real-world applications. We also studied the impact of various layouts of transmitter deployment on positioning accuracy. Our current solution has been validated only when the receivers are not tilted (i.e., are orthogonal to the

floor). In precision-demanding industrial scenarios, this requirement can be achieved by placing the receiver carefully on top of the robots. We believe our methods can offer valuable insights applicable to diverse scenarios with distinct positioning accuracy targets. Also, they can provide guidance for optimizing the deployment of LEDs to achieve the required positioning accuracy.

REFERENCES

- [1] W. Du et al., "Uniloc: A Unified Mobile Localization Framework Exploiting Scheme Diversity," *IEEE Trans. Mobile Computing*, 2020.
- [2] K. Chintalapudi et al., "Indoor Localization Without the Pain," *Proc. ACM MobiCom*, 2010.
- [3] D. Chen et al., "Locating and Tracking BLE Beacons With Smartphones," *Proc. ACM CoNEXT*, 2017.
- [4] W.-H. Kuo et al., "An Intelligent Positioning Approach: RSSI-Based Indoor and Outdoor Localization Scheme in Zigbee Networks" *Proc. IEEE ICMLC*, 2010.
- [5] L. Barbieri et al., "UWB Localization in a Smart Factory: Augmentation Methods and Experimental Assessment," *IEEE Trans. Instrumentation and Measurement*, 2021.
- [6] Torres-Sospedra et al., "Comprehensive Analysis of Distance and Similarity Measures for Wi-Fi Fingerprinting Indoor Positioning Systems," *Expert Systems with Applications*, 2015.
- [7] Seco-Granados et al., "Challenges in Indoor Global Navigation Satellite Systems: Unveiling Its Core Features in Signal Processing," *IEEE Signal Processing Mag.*, 2012.
- [8] A. Gradim et al., "On the Usage of Machine Learning Techniques to Improve Position Accuracy in Visible Light Positioning Systems," *Proc. IEEE Symposium on Commun. Systems, Networks & Digital Signal Processing*, 2018.
- [9] P. Du et al., "Demonstration of a Low-Complexity Indoor Visible Light Positioning System Using an Enhanced TDOA Scheme," *IEEE Photonics J.*, 2018.
- [10] S. Zhang et al., "3D Indoor Visible Light Positioning System Using Rss Ratio With Neural Network," *Proc. IEEE Opto-Electronics and Commun. Conf.*, 2018.
- [11] Abou-Shehade et al., "Accurate Indoor Visible Light Positioning Using a Modified Pathloss Model With Sparse Fingerprints," *J. Lightwave Technology*, 2021.
- [12] Knudde et al., "Data-Efficient Gaussian Process Regression for Accurate Visible Light Positioning," *IEEE Commun. Letters*, 2020.
- [13] X. Sun et al., "RSS-Based Visible Light Positioning Using Nonlinear Optimization," *IEEE Internet of Things J.*, 2022.
- [14] Aparicio-Esteve et al., "Experimental Evaluation of a Machine Learning-Based RSS Localization Method Using Gaussian Processes and a Quadrant Photodiode," *J. Lightwave Technology*, 2022.
- [15] Mariakakis et al., "Sail: Single Access Point-Based Indoor Localization," *ACM MobiSys*, 2014.

BIOGRAPHIES

Ran Zhu (r.zhu-1@tudelft.nl) is a Ph.D. candidate at TU Delft, Netherlands. Her research focuses on indoor positioning and embedded AI.

Maxim Van den Abeele (maximvda123@gmail.com) was a master student at KU Leuven, Belgium. His research interest is visible light positioning.

Jona Beysens (jona.beysens@csem.ch) is an R&D Engineer at CSEM, Switzerland. His research interests include tinyML and embedded systems.

Jie Yang (j.yang-3@tudelft.nl) is an Assistant Professor at TU Delft, Netherlands. He works on human-centered computing for trustworthy AI.

Qing Wang [SM] (qing.wang@tudelft.nl) is an Assistant Professor at TU Delft, Netherlands. His research interests include VLC & sensing, and embedded AI.